Concentrated slurry formation via drawdown and incorporation of wettable solids in a mechanically agitated vessel

Wood, Thomas; Simmons, Mark J. H.; Greenwood, Richard W.; Stitt, E. Hugh

DOI:
10.1002/aic.16121

Document Version
Publisher's PDF, also known as Version of record

Citation for published version (Harvard):
Wood, T, Simmons, MJH, Greenwood, RW & Stitt, EH 2018, 'Concentrated slurry formation via drawdown and incorporation of wettable solids in a mechanically agitated vessel', *AIChE Journal*, vol. 64, no. 5, pp. 1885-1895. https://doi.org/10.1002/aic.16121

Concentrated Slurry Formation via Drawdown and Incorporation of Wettable Solids in a Mechanically Agitated Vessel

Thomas Wood
Johnson Matthey Technology Centre, Johnson Matthey, Belasis Avenue, Billingham, TS23 1LB, U.K.

School of Chemical Engineering, University of Birmingham, Birmingham, B15 2TT, U.K.

Mark J. H. Simmons and Richard W. Greenwood
School of Chemical Engineering, University of Birmingham, Birmingham, B15 2TT, U.K.

E. Hugh Stitt
Johnson Matthey Technology Centre, Johnson Matthey, Belasis Avenue, Billingham, TS23 1LB, U.K.

DOI 10.1002/aic.16121
Published online February 23, 2018 in Wiley Online Library (wileyonlinelibrary.com)

This article describes the effect of vessel configurations on the drawdown and incorporation of floating solids to prepare concentrated alumina slurries in stirred tanks. The impeller speed and power draw required to incorporate all dry powder within four seconds, N_{JI} and P_{JI}, are used to evaluate incorporation performance. The effect of impeller type is assessed, with pitched blade impellers proving to be the most effective across the full range of solid contents considered. At higher solids content the energy demand is shown to increase dramatically, with a 100-fold increase in energy required to add 1% w/w more solid at 50% by weight compared to 1% by weight. Analysis of impeller power numbers show this coincides with a transition from constant power number to a region where power number increases linearly with decreasing Reynolds number. Contrary to studies at low solids content, the presence of baffles is shown to inhibit drawdown. © 2018 The Authors AIChE Journal published by Wiley Periodicals, Inc. on behalf of American Institute of Chemical Engineers *AIChE J*, 64: 1885–1895, 2018
Keywords: suspensions, drawdown, floating solids, stirred tank

Introduction

The drawdown of floating solids is a widely used operation across the process industries, whether for dissolution, reaction, or simple suspension involving the incorporation of solid into liquid. The process of incorporating solids into liquid can include some or all of the following steps, depending on the specific properties of the particles and unit operation in question:[1]

1. Wetting
2. Drawdown or submersion of the particles
3. Dispersion
4. Off-bottom suspension
5. Deagglomeration
6. Dissolution

Due to the nature of the system the solid may float for a number of reasons.[2] The first and most obvious of these is the case where the solid has a lower density so the buoyancy force on the solid particles will be greater than the gravitational settling force and cause them to float. Drawdown of these particles is steady-state phenomena and thus they will rise back to the surface if agitation ceases. Another possibility is that an agglomerate containing multiple particles with a solid envelope density higher than the liquid may have a lower bulk (overall) density than the liquid due to trapping of air between individual particles. Finally, high liquid surface tension or poor solid wettability leads to a high interfacial tension, which can result in sufficient force to overcome the gravitational settling force. In the case of these latter two phenomena, which can both occur simultaneously, incorporation is an irreversible process as the particles will be dispersed into suspension and will not rise to the surface unless the first case is also true.

Previous studies[3–10] have largely focused on finding an optimum geometry or set of conditions to achieve the most effective drawdown performance. This performance is generally measured by observation as the impeller speed to just drawdown the particles (N_{JD}), ensuring that none spend longer than four seconds on the vessel surface.[11] This is analogous to the Zwietering condition used in the suspension of sinking solids.[12] Although, it is possible to make this analogy, it is worth noting the abundance of literature available studying the suspension of solids, while there is a relative dearth of works

Correspondence concerning this article should be addressed to E. H. Stitt at hugh.stitt@matthey.com.

looking at the incorporation of floating solids. This is likely because the deformable free surface at the top of a stirred vessel significantly complicates the situation compared to the vessel bottom. Particles also have a tendency to clump and agglomerate when not dispersed in a continuous phase, which can significantly complicate the force balance on the solid.[13]

All these previous studies conclude that radial impellers are not effective for the drawdown of floating powders, being outperformed by axial and mixed flow impellers; this is another similarity to work on suspension. Generally, mixed flow pitched blade impellers (PBTs) outperform hydrofoils and other axial flow impellers, with the majority of focus on down-pumping mode of operation. Özcan-Taşkin et al.[6] show that up-pumping impellers required a significantly lower power to achieve the same drawdown performance as down-pumping impellers. This is attributed to the different drawdown mechanisms, with stronger surface turbulence giving drawdown with the up-pumping mode compared to the large vortex or recirculation loops for the down-pumping mode. Khazam and Kresta[11] also suggested different mechanisms of drawdown including the central vortex; which was shown to trap solids just below the liquid surface, turbulent engulfment; where eddies pull particles into the flow, and mean drag; where strong liquid circulation drags particles to the walls or impeller shaft where they are drawn down. Turbulence is shown to be the main mechanism of drawdown for low submergences and mean drag for higher submergences for both up and down pumping impellers.

There is a general consensus amongst previous work that baffles improve drawdown performance, although there is some variation in choice of baffle type. Hemrajani[3] recommended the use of four full length narrow baffles with width B/T of 0.02. Özcan-Taşkin and McGrath[7] show that four full baffles out perform a single or two baffles, as did Karcz and Mackiewicz,[14] specifically for up-pumping impellers. Khazam and Kresta[5] developed a novel geometry specifically for drawdown with four surfaces only baffles, which increase surface turbulence. This was done to promote drawdown whilst minimizing recirculation flows lower in the vessel, greatly reducing the power requirement for drawdown. Siddiqui[15] also recommended the use of surface only baffles, but used three rather than four.

Many researchers have considered the effect of impeller diameter, specifically the impeller diameter to tank diameter ratio (D/T). Özcan-Taşkin and Wei[8] demonstrated that impellers with a D/T of 0.33 required a higher impeller speed than larger impellers to achieve the same drawdown performance, but achieved this at lower power draw. This was true except for cases where the larger impellers drew a very large vortex, where the air entrainment lowered the power draw of the impeller. Khazam and Kresta[5] found that larger impellers ($D/T = 0.5$) outperformed smaller ones both in terms of N_{JD} and P_{JD} for their system involving slightly higher solid contents.

Scale up of mixing duties generally considers measurements made by keeping geometric similarity between two scales and comparing the measured data while maintaining constant dimensionless numbers. These dimensionless numbers show the difference between the relative importance of the impeller diameter (D) and impeller speed (N).[16] Hemrajani, and Joosten et al.[3,4] both considered the effect of scaling on low solid content drawdown processes using a down-pumping PBT with specific baffling; using one or two surfaces only baffles. Both works conclude that scaling at constant Froude Number is the most reliable method to predict scale up. Özcan-Taşkin[6] studied the scale up of a drawdown process from $T = 0.61$ m to $T = 2.67$ m for both up- and down-pumping impellers. They found that Froude Number was the most accurate predictor for down-pumping mode, although only within $\pm 30\%$ and it could not predict effects of other geometric parameters. Constant power per unit volume was shown to be the best predictor for upward pumping impellers.

Most information available in the literature focuses on cases with low solid concentrations of low particle density solids, as this is the simplest case for drawdown and most likely to give meaningful correlations. This allows measurement of N_{JD} and P_{JD} at steady state. Khazam and Kresta[5] considered the effect of increasing the amount of solids present in the system, up to a maximum of 10% by volume, using expanded polystyrene. They demonstrated a significant increase in N_{JD} from 2% to 10% although trends between impeller types were preserved as the solid content increased with both up- and down-pumping impellers requiring a similar increase in impeller speed. The solids studied were nonwettable, low density solids so it was not possible to ascertain the effect of incorporated solids at higher solid contents.

The effect of solid concentration on rheology has been shown to be very significant. For rigid spheres the relative apparent viscosity of suspension increases exponentially with increasing solid concentrations up to the maximum packing fraction according to the Krieger Dougherty model.[17] Concentrated monodisperse suspensions of spherical particles have also been shown to display yield stresses above volume concentrations of 0.5.[18] Both these phenomena have been shown in less regular solid suspension, although the degree to which they occur and point of onset highly depends on the type, shape and size of the particles considered.[19]

In this article, the drawdown of floating solids up to 50% weight is studied for five different common impeller types at two scales (5 and 25 L, a five-fold volume increase) and for different baffle geometries. A similar approach to many of those works described above is used. However, rather than low true density particles and steady state drawdown conditions, alumina powder is used; for which drawdown and wetting is an irreversible process as the powder is incorporated into a slurry. The alumina powder is porous and floats initially on the liquid surface and must be mechanically drawn down and incorporated. Once this happens the impeller disperses agglomerates, freeing trapped air and the pores fill with fluid. Once fully incorporated the powder sinks if agitation ceases. This allows measurement at increasing solid contents as the concentration of the slurry is increased, demonstrating both the effect of higher solids on drawdown and interactions between solid content and impeller or geometry choice. The novelty and importance of this study is that it enables understanding of industrially relevant slurry systems where the drawdown of floating powders acts as a significant technical challenge in formulation preparation. For example; many coating formulations such as decorative paints, catalyst wash coats and fuel cell electrodes commonly use high solid content slurries, often up to and above 40 wt %.

Experimental

Two scales of flat bottomed cylindrical vessel with diameters, $T = 0.17$ m (5 L) and $T = 0.32$ m (25 L) were used in this study. These were both filled to an initial height, $H = T$, geometrical parameters are shown in Figure 1. At the smaller scale, five different impellers were used with Torrance sawtooth and 6 bladed Rushton disc turbine (RDT6) impellers as example radial flow impellers, up- and down-pumping pitched blade impellers

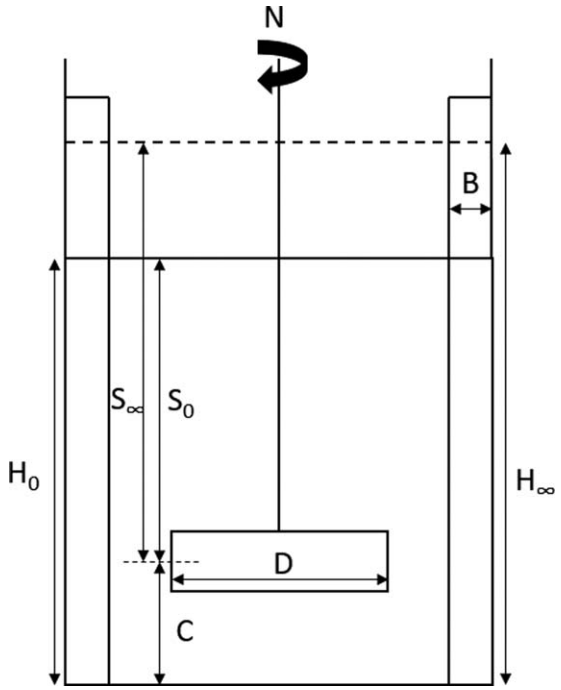

Figure 1. Vessel Schematic.

(UP-PBT4 & DP-PBT4) as mixed flow impellers and a down-pumping Lightnin A310 hydrofoil as a purely axial flow impeller as shown in Figure 2.[20] Four baffle configurations were considered: unbaffled, full, surface and bottom half. In all configurations with baffles the baffle width, $B/T = 0.1$. At the larger scale only the unbaffled case was considered for up-and down-pumping PBTs. The effect of moving the impeller to an eccentric (off-axis) position by 0.1T was also considered as a way of reducing full body rotation without using baffles.[21]

For all five impeller types, three sizes of impeller were used, corresponding to a D/T of 0.25, 0.33, and 0.5. The impeller blade thickness was kept constant between scales at 1 mm. The effect this has on power number has been shown to vary for impeller type, being significant for RDT impellers although not for PBT impellers.[22] However, this effect will be minimal with the relatively small change in scale, especially compared to the significant change in power draw due to changing solid content.

The majority of results presented are for unbaffled, centrally mounted impellers with an initial submergence, S_o of 0.5T unless otherwise stated. Submergence is measured to the middle of the impeller, as shown in Figure 1.

To give an initial fill height of $H = T$ the vessel was filled with 3.86 L solution at the small scale and 25.7 L at the large scale. An equal mass of solid was used to give a final solid concentration (X) of 50% w/w. The solid used was Sasol Puralox SCFa-140, a γ-alumina, added up to 50% in 50 aliquots, this allowed measurement at increasing solid concentration. These aliquots were 77 g at the small scale and 514 g at the larger scale and were prepared prior to the start of the experiment using a KTron KT20 loss in weight powder feeder set to deliver a fixed mass. Solid was added in this manner to give sufficient measurements to show the effect of increasing solids content. It also ensured enough solid was added in each aliquot to completely cover the liquid surface when the impeller was at rest. The alumina is a porous ceramic material and initially floats on the liquid surface. However, once wetted and fully incorporated, if the slurry is not agitated, the solid will sediment to the bottom of the vessel, rather than return to the surface.

The liquid used in these experiments was a dilute (initially 6% by weight) aqueous acetic acid solution to give a final (50 wt %) slurry pH of <5. This was required to prevent the pH approaching the isoelectric point of the slurry at high solids content; this would have a very significant impact on the viscosity, causing the slurry to gel and so it was necessary to avoid this. The isoelectric point for the γ-alumina is in the range 7.7–7.9.[23]

The point at which the solid is just drawn down and incorporated was measured visually by observing the point at which no solid remains dry on the liquid surface for longer than four seconds. This operating condition is termed *Just Incorporated* (N_{JI}) and is similar but distinct from the *Just Drawdown* (N_{JD}) condition reported in other works.[3–10] This distinction is made as, in this case N_{JI} does not represent a steady state condition as once the powder is incorporated it will not become dry and float again, as is the case with solids in previous studies.

The H/T in the vessel increased as solid was added to a maximum of approximately 1.2 at 50% by weight of solid.

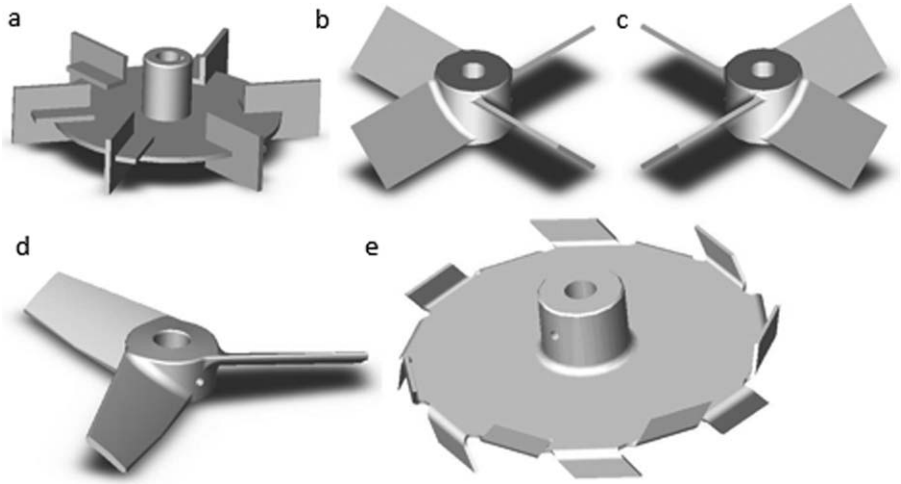

Figure 2. Selection of impellers studied. 6 bladed Rushton disc turbine (a), down pumping pitched blade (b), up pumping pitched blade (c), Lightnin A310 hydrofoil (d) and sawtooth impeller (e) (Post Mixing Optimizations and Solutions, 2017.

Table 1. N_{JI} & P_{JI} for Initial and Final H/T & S/T for High and Low Solid Contents

Condition	N_{JI} (RPM)	P_{JI} (W)
$H/T = 1$, $S/T = 0.5$, $X = 0\%$	210	0.11
$H/T = 1.2$, $S/T = 0.7$, $X = 50\%$	590	23.1
$H/T = 1.2$, $S/T = 0.7$, $X = 0\%$	275	0.19

Thus, the submergence of the impeller increased throughout the duration of the experiment and so a control was carried out to determine the extent to which any effects seen at high solids were caused by the solid content, rather than the increased submergence. To do this, N_{JI} was measured for the first addition of powder in the small-scale vessel with H/T = 1.2 and S/T = 0.7 (equivalent to $S_0/T = 0.5$ in the normal experimental procedure). The results in Table 1 clearly demonstrate that while increasing the liquid height and submergence will have a negative impact on drawdown, the presence of solid dominates over this, even with the change in liquid height. This control experiment was done using a down-pumping PBT with $D/T = 0.5$.

Torque (Γ) was measured using a calibrated Binsfield TorqueTrak 10k wireless strain gauge attached to the impeller shaft. Torque was then used to measure the power dissipation in the vessel as

$$P_{JI} = 2\pi N_{JI}\Gamma \tag{1}$$

The slurry rheology was measuring using a TA AR2000 rheometer with a 28 mm diameter vane and 44 mm diameter cup geometry. Measuring the rheology of quickly sedimenting solids is very difficult due to settling and it was not possible to measure the full flow curve with either geometry without the slurry separating. Thus, in place of a full flow curve the apparent viscosity of the slurry was measured at a fixed shear rate of $200s^{-1}$ for 3 min. The shear rate used was estimated as the effective shear rate in the stirred vessel using the approach described by Metzner and Otto.[24] They suggested that the effective shear rate is proportional to the impeller rotation speed

$$\dot{\gamma}_{\text{eff}} = k_s N \tag{2}$$

Where k is an impeller specific constant, ranging in this case from 10 for the PBTs to 11.5 for the RDT.[25] The highest effective shear rate seen in these experiments was using the RDT impeller at $N = 1000$ RPM. This gives an effective shear rate of approximately 200 s^{-1}. For this reason, the slurry apparent viscosity was measured at a constant shear rate of 200 s^{-1}; using the highest shear rate as it was also the most likely to prevent sedimentation during the rheological measurement.

This apparent viscosity was used to calculate the Reynolds number of the vessel at the Just Incorporation condition such that

$$Re_{JI} = \frac{\rho N_{JI} D^2}{\mu_{\text{app}}} \tag{3}$$

The root means square error (RMSE) is used to compare the reliability of the different scaling parameters studied calculated as

$$\text{RMSE} = \sqrt{\frac{1}{50}\sum \left(N_{\text{Large, measured}} - N_{\text{Predicted}}\right)^2} \tag{4}$$

Where the measured and predicted impeller speeds are specific to each of the 50 powder additions.

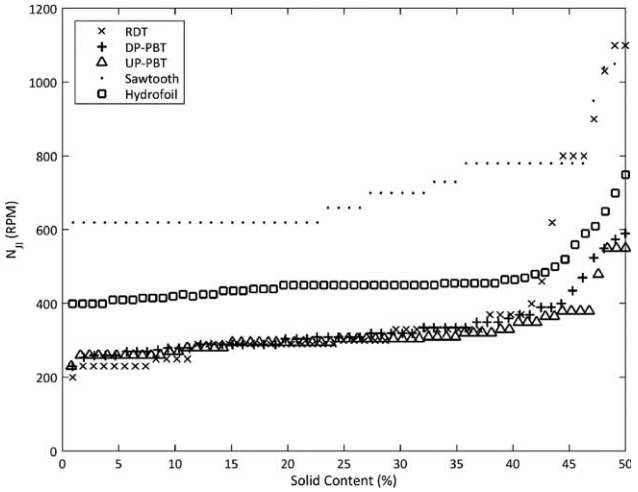

Figure 3. Vessel surface showing incorporation via a vortex (a) and large agglomerate at impeller after vortex collapse (b).

Results and Discussion

Effect of pumping mode, impeller type and solid concentration

In Figure 3, the impeller speed for just incorporation for the five impeller types tested at a D/T of 0.5 is shown. In all cases, N_{JI} increases with increasing solid content as it becomes harder to draw down and incorporate more solid from the surface at higher solid loadings. This effect becomes particularly pronounced at around 40% by weight solids for all impellers of this size. It is also around this point that there is a significant increase in the impeller power draw, as shown in Figure 4. It was observed that this dramatic increase in N_{JI}, typically at $40 \pm 5\%$ w/w solids that generally also coincided with the collapse of the vortex pulled by the impeller. At this point the incorporation mechanism changed. At low solid contents with a large vortex the dry powder was pulled down through the vortex to the impeller, from which it is then dispersed into the suspension. As the vortex collapsed at higher solids, added solid tended to clump on the liquid surface and form agglomerates which would partially wet, becoming sufficiently dense

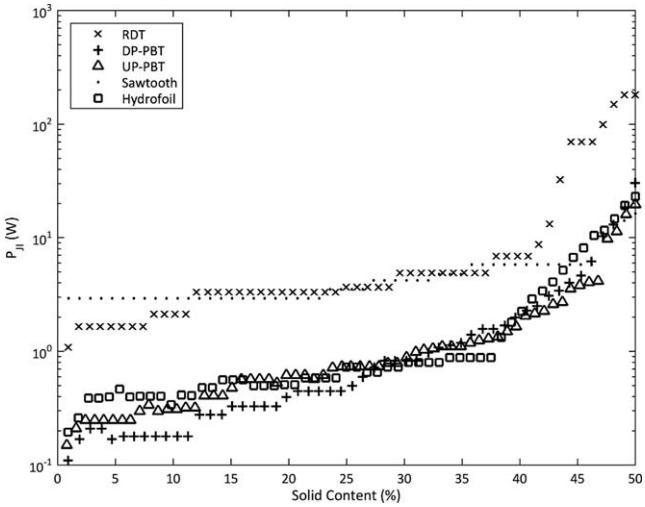

Figure 4. N_{JI} with increasing solids content for different impeller types, all with $D/T = 50\%$ and $S_0/T = 50\%$.

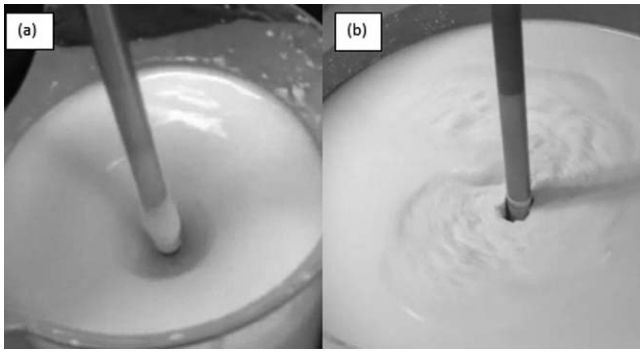

Figure 5. P_{JI} with increasing solids content for different impeller types, all with $D/T = 50\%$ and $S_0/T = 50\%$.

to sink below the surface and physically hit the impeller to become dispersed, this is much more akin to the mean drag mechanism of drawdown described by Khazam and Kresta.[11] Example images of this transition are shown in Figure 5.

The sawtooth, as the impeller with the lowest pumping number and having a radial flow pattern,[26] required the highest N_{JI} at low solids concentration. The mixed flow PBT impellers are shown to be the best performing, requiring both the lowest speed and power draw across the full range of solid contents tested. The PBTs significantly out-perform both the radial flow impellers, in terms of speed and power required for drawdown, and marginally out-perform the more axial flow hydrofoil, regardless of pumping direction. This result is similar to the low solid concentration studies described above and seems to hold true even at the higher solid contents studied here.

The RDT was most significantly affected by the presence of solids in the vessel, with significant increases in N_{JI} being seen above ~37% w/w solids, whereas in contrast, the PBTs only started to show significant increases above 45% w/w. The sawtooth impeller showed the highest resilience to solid concentration. This is especially true in terms of power consumption where, although at low solids it performed similarly to the RDT (also a radial impeller) it did not demonstrate the very

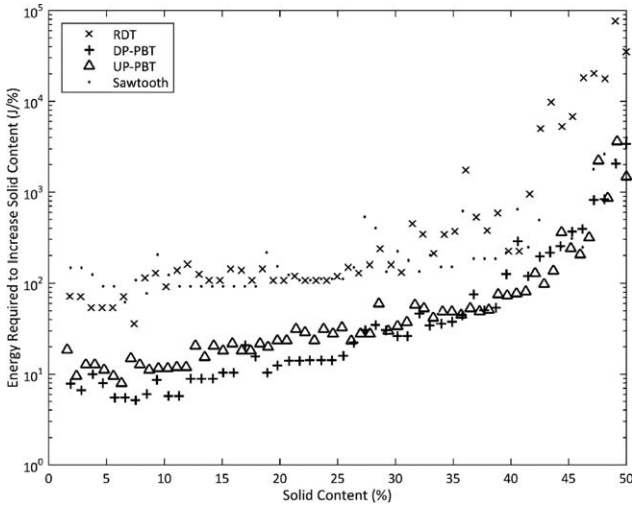

Figure 6. Energy required to increase slurry solid content by 1% with increasing solid content for different impeller types, all with $D/T = 50\%$ and $S_0/T = 50\%$.

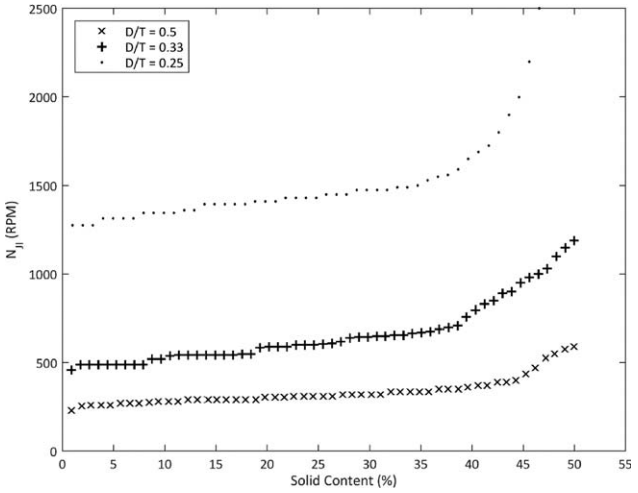

Figure 7. Comparison of N_{JI} with increasing solid content for three sizes of down pumping PBT.

significant rise in N_{JI} and P_{JI} until a significantly higher solid content. This suggests that as the suspension becomes more rheologically complex with higher solids loadings the high shear rate imparted by the sawtooth in the impeller region has a beneficial effect, despite the low pumping number. This is likely caused by more effective breakup of the agglomerates forming at the surface after the vortex collapses.

Although this demonstration that mixed flow impellers outperform their radial and axial counterparts is similar to previous works it is important to note the dramatic increase in P_{JI} with increasing solid content. The increase in N_{JI} combined with this significantly larger impeller shaft torque means that increasing the solid content of a slurry by a further 1% requires almost 100-times as much energy for a 50% by weight slurry compared to a 1% by weight suspension as seen in Figure 6. The dramatic increase in impeller shaft torque is a combined effect of the increased impeller speed and the dramatic increase in viscosity, as expected due to the Krieger Dougherty relationship.[17]

Effect of impeller size

For all impeller designs tested the smallest impellers struggled to maintain incorporation of powder at the highest solid contents. The measured impeller speed required for incorporation increased faster for the smallest impellers than for the larger impellers, as shown for a down pumping PBT in Figure 7. This was so extreme that for all $D = 0.25$ T impellers the impeller speed required to maintain drawdown and incorporation within four seconds exceeded 2500 RPM, which was the maximum speed possible with available motors, before the target of 50% w/w solid was attained.

The impeller power draw determined from shaft torque measurements, shown in Figure 8, showed very similar performance between different impeller sizes across most solid contents, with the largest impeller requiring the least power at the lowest solid contents which matches observations by.[5] This suggests that, within normal size ranges, larger diameter impellers are likely to outperform smaller ones as they will require a lower impeller speed to maintain the same incorporation performance. This, generally, will give more flexibility in a process to increase the speed further to push to higher solids content if required.

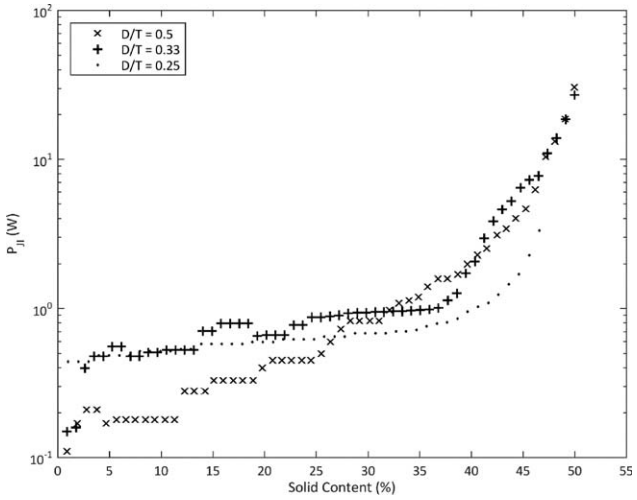

Figure 8. Comparison of P_{JI} with increasing solid content for three sizes of down pumping PBT.

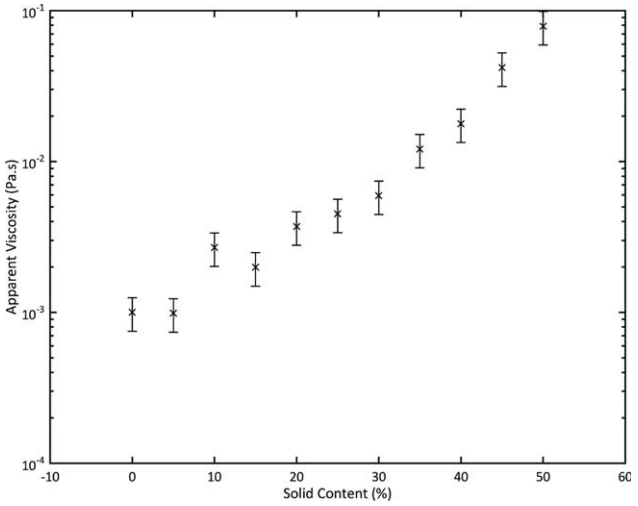

Figure 10. Evolution of slurry apparent viscosity for increasing solid content. Measured at $200s^{-1}$.

Effect of baffles and eccentricity

In many previous studies considering drawdown of low density, nonincorporable solids, baffles were found to improve drawdown performance. However, as shown in Figure 9, this was not found to be the case with solids that are incorporated. Adding baffles provided extra surface area at the surface to which the dry powder became caught behind. This dry powder acted as a site of agglomeration for more powder on the surface, forming a motionless semiwet mass that could not be drawn down. This was especially true in the dead zones behind the baffles; where, for additions above approximately 20% by weight, dry powder quickly collected. This dry powder then became partially wetted by the liquid and formed a large stationary agglomerate which became very difficult to drawdown for incorporation to occur. This meant that maintaining the Just Incorporation condition quickly became impossible for both full and surface baffles, where metal protruded above the liquid surface.

Bottom half baffles marginally improved the drawdown performance at the lowest solid contents.

However, as the solid content increased the impeller speed for drawdown increased much more

significantly than in the unbaffled cases, again decreasing drawdown efficiency as the solid content was increased further. This is due to the fact that the presence of baffles prevented vortex formation within the vessel, which inhibited wetting and incorporation of the powder.

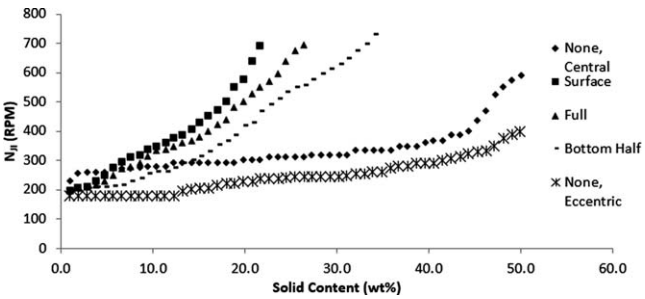

Figure 9. Effect of baffle geometries and impeller eccentricity on N_{JI} for down pumping PBT with $D/T = 0.5$.

Significantly higher shaft torque was also seen in the eccentric, full, and bottom half baffle cases at the low solids contents studied, this is to be expected as the centrally mounted impeller showed a high degree of bulk rotational flow, which will reduce the energy dissipation by the impeller due to a lower power number. This is not true in the fully baffled case. This has implications for the mixing performance as it is possible that, although drawdown efficiency is increased in the unbaffled cases, the mixing performance will be reduced, increasing the chances of inhomogeneity in the vessel. This limitation was overcome through use of an eccentric impeller, which gave a noticeably higher power draw (with a measured power number of 1.3 at low solid contents, whereas the central impellers had a power number in the region 0.3–0.4) and better drawdown performance. These observations were observed for both up and down pumping PBTs at a variety of submergences.

Flow regimes

There is a significant change in drawdown behavior at around 40% solids by weight, although the exact concentration at which this happens is impeller specific. In order to explore this observed step change in behavior the apparent flow regime within the vessel was studied by considering the Reynolds and power numbers of the system around the transition.

The apparent viscosity of the slurry was measured as described above. As seen in Figure 10 the slurry apparent viscosity increased exponentially with the solid content. Both the hatched plate and vane geometries give similar apparent viscosities to $\pm 15\%$. Fitting an exponential to these measurements gives the apparent viscosity at 200 s^{-1} as a function of solid content for $0\% \leq X \leq 50\%$:

$$\mu_{app} = 0.0006e^{0.0994X} \tag{5}$$

The rheology of the slurry was measured in this manner because it is extremely difficult to measure full rheology curves. This is because at low shear rates the slurry separated within seconds, displacing the water and causing the solid to dry out during measurement. However, it was observed during mixing that even at the highest solid contents and large initial submergence, a dry particle placed near the wall at the free

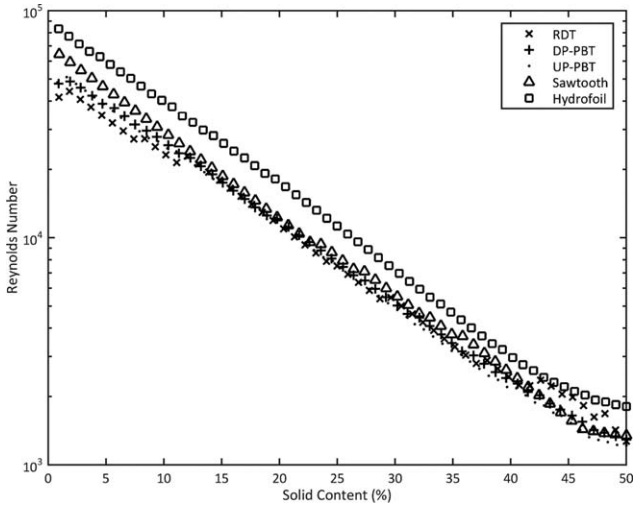

Figure 11. Evolution of Reynolds number in the vessel as the solid content increased for all impellers studied with $D/T = 0.5$.

surface would move, tracing the liquid flow. As the point in the vessel furthest from the impeller motion of fluid to the impeller from the wall at the surface shows that the slurry was fully mobile, with no caverns forming.

Figure 11 shows that the Reynolds number steadily decreases with increasing solid content as the slurry becomes more viscous, despite the increasing impeller speed. At ca. 40% w/w solids, where the apparent change in incorporation mechanism occurs, all impellers seem to have a Reynolds number in the order of 2000–3000. This would classically be considered to be inside the transitional regime but not close to the laminar transition, which is generally accepted to occur at around Re = 10. The transition from full turbulence to transitional flow, based on the commonly assumed boundary of ca. Re = 10,000, would occur between 25 and 30% w/w solids.

The impeller power number can be calculated from the measured power draw as

$$Po = \frac{P}{\rho N^3 D^5} \tag{5}$$

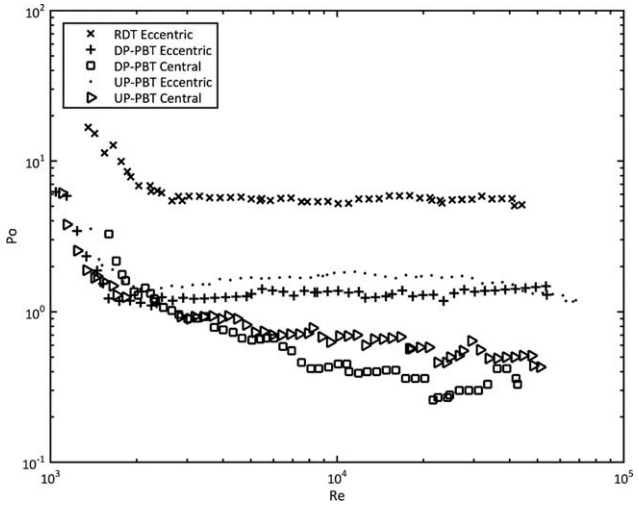

Figure 12. Change in impeller power number for change in Reynolds number & solid content for RDT, up & down pumping PBT.

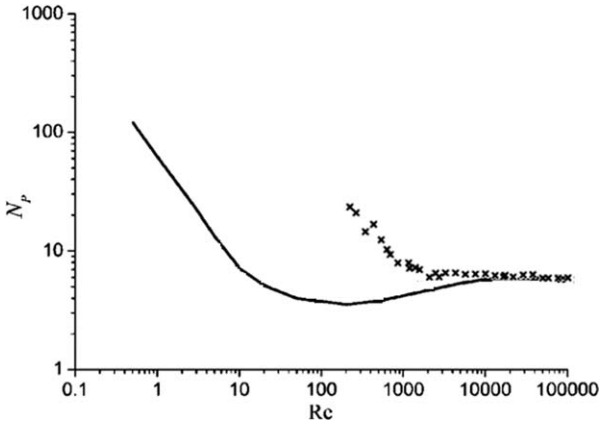

Figure 13. Measured power numbers for Rushton turbine compared to standard values (24).

Figure 12 shows that the power number remained constant as the Reynolds number dropped from its maximum, at the start of the experiments, with no solids present to a Reynolds number of 2000. This constant Po with changing Re is indicative

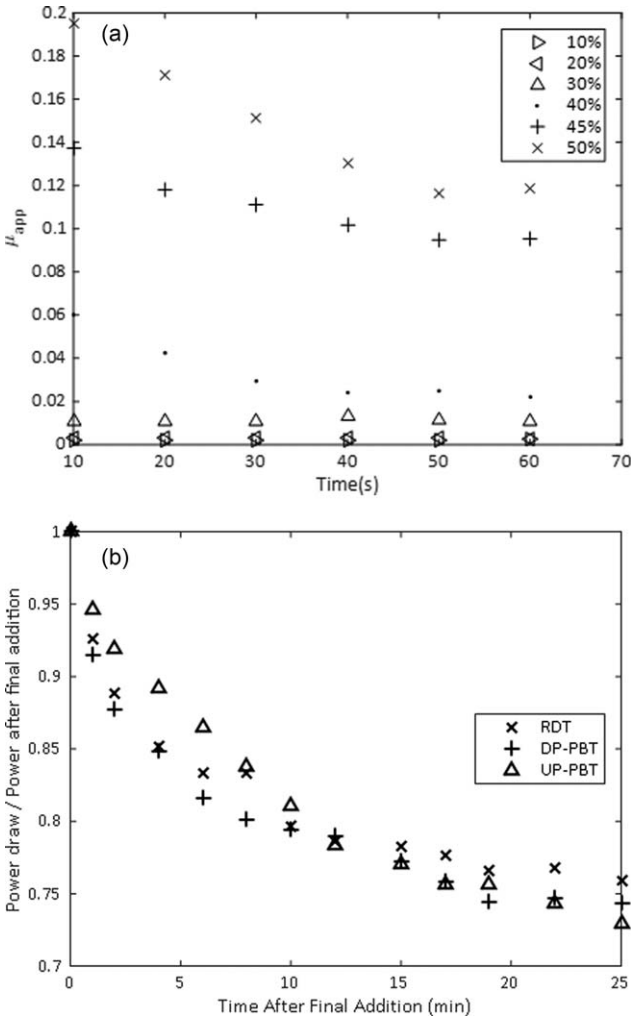

Figure 14. Rheology evolution shown by apparent viscosity measurements of freshly made slurry held in a 40 mm vane rheometer for 1 min at 200 s^{-1} (a) and shaft torque changes in the mixing vessel (b).

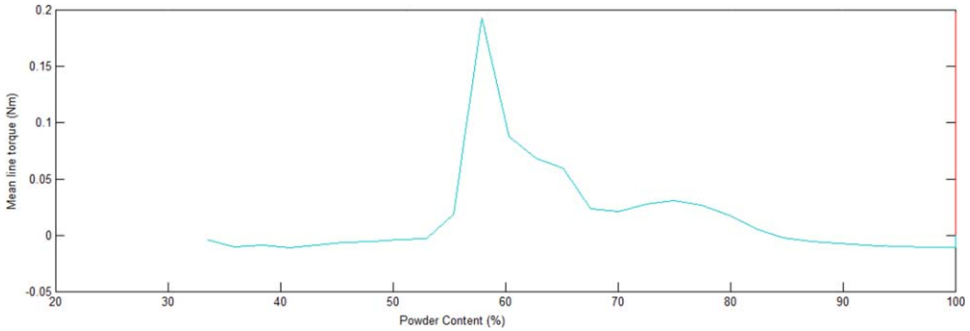

Figure 15. Mixer torque rheometry plot for alumina slurry.

[Color figure can be viewed at wileyonlinelibrary.com]

of fully turbulent flow. The value of the power number is also approximately 1.3 for the PBTs and 5 for the RDT, the power numbers expected for a fully turbulent pitched blade impeller and Rushton turbine.[25,27] From Figure 11 this Reynolds number value coincides with a solid content of approximately 40%. At solid contents above this (and lower Reynolds numbers) the power number increases with decreasing Reynolds number, indicative of laminar flow, explaining the collapse of the vortex and massive increase in requirement to maintain effective drawdown and incorporation.

Figure 13 compares the measured power numbers to standard values for a Rushton turbine.[27] The figure illustrates that the presence of the solids appears to suppress the transitional regime, causing a prolongation of the "laminar" flow regime, where a linear increase in power number with decreasing Reynolds number is observed.

Possible reasons for this phenomenon are local or bulk changes in the rheology of the fluid due to complex dynamic interactions between the liquid and solid particles (as well as possible particle-particle interactions) or that the solids particles act to suppress turbulence within the continuous phase. Suppression or augmentation of turbulence within solid–liquid and liquid–liquid systems is an observed phenomenon which has been the studied by many workers at low dispersed phase concentrations,[28–31] although mechanistic understanding at high solids concentrations remains elusive with little study.[32]

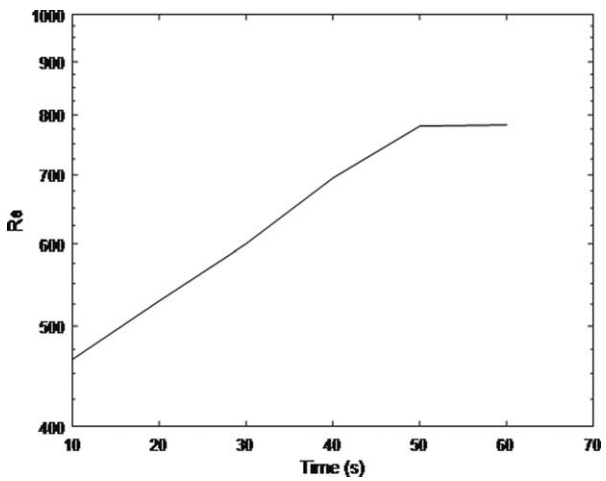

Figure 16. Calculated Reynolds number change due to evolution in apparent viscosity with processing time for 50 wt % slurry held in vane rheometer.

Evidence exists in the rheology data of unstable behavior at high solid loadings. This is shown in Figure 14a where crude slurry was held in the vane rheometer for one minute at 200 s^{-1}. For slurries with solid content $\geq$40 wt % the rheology evolved with processing time, and the apparent viscosity decreased; this is likely due to deagglomeration of small agglomerates that remain after large agglomerates are broken up directly by the impeller. These small agglomerates contain occluded air, and so give the slurry a temporary artificially high solid volume concentration. The apparent viscosity values used to calculate Reynolds number above were once the slurry reached a steady μ_{app} after more than a minute.

Figure 14b shows that the same rheology change occurred in the vessel when the slurry was agitated in the vessel at constant impeller speed, as seen by a decrease in power draw (normalized by the initial value) with time. For all impellers, the value of power draw decayed to around 75% of the initial value, following immediately after the final powder addition, within 20 min.

This artificially high solid volume concentration due to occluded air causes the slurry to act as a more concentrated slurry, moving further to the right in the mixer torque rheometry curve for this powder, shown in Figure 15. This means the slurry acts more like a paste and so has a lower Reynolds number whilst deagglomeration is still occurring, due to the increased viscosity. Figure 16 shows how the Reynolds number increases as the viscosity decreases with deagglomeration time as the occluded air is released.

Scale up

Six scales up protocols were considered: Constant N^3D, constant tip speed, constant impeller discharge, constant Froude Number, constant Reynolds number, and constant power per unit volume, the dependencies of which are shown in Table 2.

The protocols are listed in descending dependence on the impeller speed from the highest (N^3D) to the lowest

Table 2. Scaling Protocols Considered

Scaling Protocol	Constant	Assumed Inter-Scale Constants
Froude number*N	N^3D	–
Froude number	N^2D	–
Power per unit mass	N^3D^2 (turbulent) N (laminar)	Impeller power number (turbulent)
Tip speed	ND	–
Reynolds number	ND^2	Fluid viscosity & density
Flow	ND^3	Impeller flow number

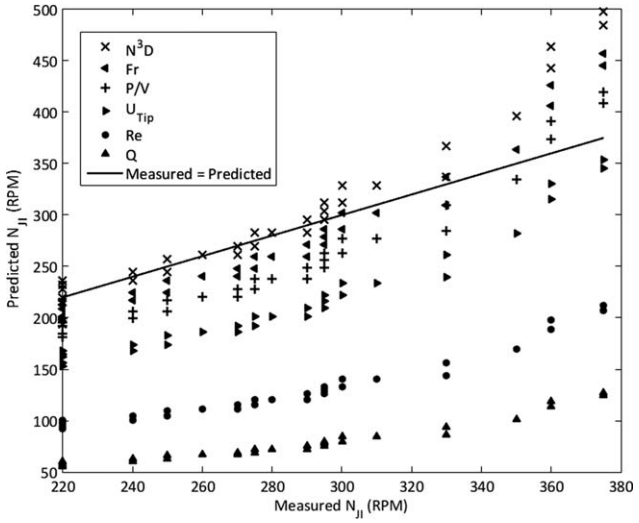

Figure 17. Predicted vs. measured N_{JI} values for scaling protocols.

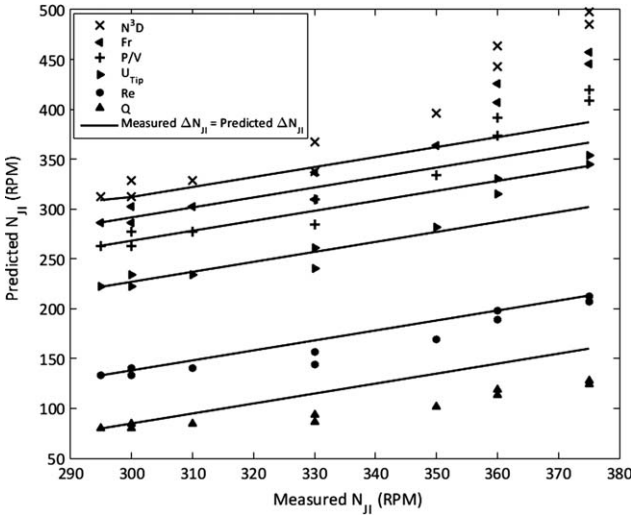

Figure 18. Predicted vs measured N_{JI} values for down pumping PBT at >40 wt % solids with lines showing how each scaling protocol predicts ΔN_{JI}.

(flow, ND^3). Although it is worth noting that the regime change observed above will affect some of these parameters. For example, Froude number is generally relevant to systems containing a vortex. In this work the vortex was observed to collapse at 40 wt % solids and so it is unlikely that Froude number will be relevant beyond this point. Similarly, constant power per unit mass is dependent on a constant power number in turbulent flow to give a dependency on N^3D^2. However, as the flow becomes laminar Po is no longer constant so constant power per unit mass becomes dependent on a constant Po.Re, or a constant N.

The approach used was to measure the value of N_{JI} with increasing solids for down pumping PBTs at both large and small scale. The small-scale values were then used to predict large scale values based on each of the above scaling parameters. The predicted and measured values were then compared.

Figure 17 shows that maintaining a constant N^3D between scales is the best scaling protocol for the lowest solid contents, giving the lowest RMSE shown in Table 3. However, as the solid content of the slurry is increased the ability of any of the parameters to predict scale up fails. This point corresponds to the regime transition at 40% by weight solid observed above.

This is a different result to previous studies[3,4,6] which generally showed a constant Froude number to be the best scaling protocol for drawdown. This result shows extra dependency on the impeller rotation speed compared to Froude number: thus, the scaling parameter proposed is N.Fr. While it is not surprising to find that the Froude number is an important parameter[3,4,6] the extraneous "N" deserves a little more discussion.

There are two possible explanations, both of which are essentially variants on a similar theme:

1. Average Shear (Metzner and Otto (8), and Eq. 2 above) = K_S.N. Given the same impeller is used at both scales, then K_S = constant so the average shear α N. Although, this approach is only applicable for laminar flow, it is included as a possible explanation here given that the laminar flow regime in this work appears to have been prolonged (Figure 13).

2. Whole vessel pumping: Q = Fl. ND^3 so vessel turnover frequency is proportional to Fl. ND^3/T^3. Given that D/T = constant as geometric similarity is maintained and that Fl = constant as the same impeller is used at both scales, then scale independent whole vessel turnover frequency α N

Scaling of N.Fr, therefore, considers not only the drawdown, courtesy of Fr, but also the ability to distribute the incorporated solids around the vessel, or alternatively the ability to maintain average shear rates that could reflect the disruptive forces on the drawn down agglomerates or the suppression of cavern formation.

Figure 17 shows that none of the scaling protocols suitably predict scale up after the regime change when considered as part of the full range of concentrations. However, it is possible to predict the change in impeller speed after the regime change where:

$$N_{2,\text{Predicted}} = \left(\frac{\left(N_{1,\text{Measured}} - N_{1,\text{Transition}}\right)^a D_1^b}{D_2^b} \right)^{\frac{1}{a}} + N_{2,\text{Transition}} \tag{6}$$

Where 1 and 2 represent the two scales considered.

Table 3. Error from Measured and Predicted N_{JI} Values for Scale Up from 5L to 25L for Down Pumping PBT

Scaling Protocol	RMSE—Full	RMSE –<40%
Froude number*N	32.29	7.44
Froude number	27.67	22.12
Power per unit mass	39.09	40.95
Tip speed	72.20	74.65
Reynolds number	152.66	147.59
Flow	202.03	191.40

Table 4. Error between Measured and Predicted ΔN_{JI} Values for different Scaling Protocols

Scaling Protocol	RMSE—ΔN_{JI} at > 40%
Froude number*N	58.30
Froude number	46.68
Power per unit mass	39.19
Tip speed	26.28
Reynolds number	10.85
Flow	24.34

The impeller speed at the regime transition is specific to the power and liquid system considered and so must be measured experimentally. The values of a and b are the values of the exponents of N and D respectively for the scaling criteria considered, shown in Table 2. Applying Eq. 6 predicts the change in N_{JI} from the impeller speed at the regime transition to the considered solid content for one of the above scaling protocols.

Figure 18 shows the change in impeller speed (ΔN_{JI}) as opposed to the absolute value of N_{JI} after the regime change using Eq. 6 above for each of the scaling protocols considered. From this a constant Reynolds number most accurately predicts ΔN_{JI}, as shown by the best match of measured ΔN_{JI} vs. predicted ΔN_{JI}. This is reflected in the RMSE values shown in Table 4.

This is a new observation, showing that the regime change observed above also changes the scaling dependence of the system. Where the impeller speed required for effective drawdown is calculated as

For constant Po (turbulent) regime

$$N_{JI,2}=\sqrt[3]{\frac{N_{JI.1}{}^3 D_1}{D_2}} \tag{7}$$

For changing Po regime

$$N_{JI,2}=N_0+\frac{\Delta N_{JI,1} D_1{}^2}{D_2{}^2} \tag{8}$$

Where 1 and 2 represent the two scales considered, ΔN is the change in impeller speed with increasing solids after the regime change, and N_0 is the impeller speed at the regime change.

This change in scaling dependency is likely caused by the change in incorporation mechanism that happens at the regime change. As stated above; below the transition loose particles are drawn down and incorporated through a vortex. After the transition mean drag of larger agglomerates, that form on the surface due to gentle surface motion, becomes the main incorporation mechanism. These two mechanisms are significantly different and therefore give rise to these two scaling regimes.

Conclusions

This work demonstrates the effect of high solid content systems on the drawdown and incorporation of floating solids in stirred vessels. Similarly, to low solid systems in previous works, the mixed flow impellers out performed either radial or axial flow impellers tested. This is true for the entire range of solid contents studied (up to 50% by weight). However, at the very highest solid contents (40%+) the mechanism of powder incorporation changed; the central vortex collapses at this point such that solid is no longer brought directly to the impeller. Instead clumps of semiwetted powder tend to form into agglomerates, these then sink below the surface as fluid motion wets them to a sufficient density to overcome buoyancy forces on them. At this point the sawtooth impellers studied went from being the worst impeller at low solids to one of the better performing ones, this suggests that high shear is beneficial in achieving very high solid contents.

Generally larger impellers (up to a max D/T of 0.5) out performed smaller ones. This was especially true for the smallest impellers studied at $D/T = 0.25$, which were often too small to produce sufficient surface motion at higher solids to sufficiently wet power to incorporate it.

Contrary to many works at low solid contents baffles were found to significantly inhibit the incorporation of powder as the solid content was increased. This was true for all types of baffles tested, with submerged half baffles being the best but still performing significantly worse than the unbaffled system. It would be interesting in further work to see the effect of moving the impeller eccentric or tilting the impeller on incorporation performance. These are generally ways to prevent full body rotation in systems where baffles are not suitable.

Scaling on a constant N^3D is found to predict most accurately the scale up from a 5 L vessel to 25 L with geometric similarity for both up and down pumping PBTs up to around 40% by weight solid content. This was the maximum concentration before the vortex collapsed in all systems tested and coincides with a constant Reynolds Number better predicting the change in impeller speed required to maintain drawdown. This concentration, approximately 40% by weight solids for this specific powder, is also where a flow transition from turbulent (or constant power number) to laminar seems to occur, which has been demonstrated by analysis of the apparent power number of the impeller at that point, which shows very little transitional flow behavior.

Acknowledgments

Thomas Wood is funded by the EPSRC Centre for Doctoral Training in Formulation Engineering at the University of Birmingham (grant number EP/L015153/1) and Johnson Matthey.

Literature Cited

1. Freudig B, Hogekamp S, Schubert H. Dispersion of powders in liquids in a stirred vessel. *Chem Eng Process Process Intensif.* 1999; 38(4–6):525–532.
2. Waghmare Y, Falk R, Graham L, Koganti V. Drawdown of floating solids in stirred tanks: scale-up study using CFD modeling. *Int J Pharm.* 2011;418(2):243–253.
3. Hemrajani RR. *Suspending floating solids in stirred tanks: mixer design, scale-up and optimization*. Pavia, Italy, 1988:259–265.
4. Joosten GEH, Schilder JGM, Broere AM. Suspension of floating solids in stirred vessels. *Trans Inst Chem Eng*. 1977;55(3):220–222.
5. Khazam O, Kresta SM. A novel geometry for solids drawdown in stirred tanks. *Chem Eng Res Des*. 2009;87(3):280–290.
6. Özcan-Taşkin G. Effect of scale on the draw down of floating solids. *Chem Eng Sci*. 2006;61(9):2871–2879.
7. Özcan-Taskin G, McGrath G. Draw down of light particles in stirred tanks. *Chem Eng Res Des.* 2001;79(7):789–794.
8. Özcan-Taşkin G, Wei H. The effect of impeller-to-tank diameter ratio on draw down of solids. *Chem Eng Sci*. 2003;58(10):2011–2022.
9. Takahashi K, Sasaki S. Complete drawdown and dispersion of floating solids in agitated vessel equipped with ordinary impellers. *J Chem Eng Jpn*. 1999;32(1):40–44.
10. Thring RW, Edwards MF. An experimental investigation into the complete suspension of floating solids in an agitated tank. *Ind Eng Chem Res*. 1990;29(4):676–682.
11. Khazam O, Kresta SM. Mechanisms of solids drawdown in stirred tanks. *Can J Chem Eng*. 2008;86(4):622–634.
12. Zwietering TN. Suspending of solid particles in liquid by agitators. *Chem Eng Sci*. 1958;8(3–4):244–253.
13. Xie L, Rielly CD, Eagles W, Özcan-Taşkin G. Dispersion of nanoparticle clusters using mixed flow and high shear impellers in stirred tanks. *Chem Eng Res Des.* 2007;85(5):676–684.
14. Karcz J, Mackiewicz B. Effects of vessel baffling on the drawdown of floating solids. *Chem Pap*. 2009;63(2):164–171.
15. Siddiqui H. Mixing technology for buoyant solids in a nonstandard vessel. *AIChE J*. 1993;39(3):505–509.
16. Stitt EH. Models of good behaviour. *Chem Eng*. 2016;901(2):33–36.
17. Krieger IM, Dougherty TJ. A mechanism for non-Newtonian flow in suspensions of rigid spheres. *Trans Soc Rheol*. 1959;3(1):137–152.

18. Heymann L, Peukert S, Aksel N. On the solid-liquid transition of concentrated suspensions in transient shear flow. *Rheol Acta*. 2002; 41(4):307–315.
19. Mueller S, Llewellin EW, Mader HM. The rheology of suspensions of solid particles. *Proc R Soc Lond Math Phys Eng Sci*. 2010; 466(2116):1201–1228.
20. Post Mixing Optimizations and Solutions. Impellers, 2017. http://www.postmixing.com/mixing%20forum/impellers/impellers.htm (accessed on 13 February 2018)
21. Hall JR, Barigou M, Simmons MJH, Stitt EH. A PIV study of hydrodynamics in gas-liquid high throughput experimentation (HTE) reactors with eccentric impeller configurations. *Chem Eng Sci*. 2005; 60(22):6403–6413.
22. Chapple D, Kresta SM, Wall A, Afacan A. The effect of impeller and tank geometry on power number for a pitched blade turbine. *Chem Eng Res Des*. 2002;80(4):364–372.
23. Adegbite SA. Coating of catalyst supports: links between slurry characteristics, coating process and final coating quality. PhD Thesis, University of Birmingham, 2010.
24. Metzner AB, Otto RE. Agitation of non-Newtonian fluids. *AIChE J*. 1957;3(1):3–10.
25. Nienow AW, Edwards MF, Harnby N. *Mixing in the Process Industries*, 2nd ed. Oxford, UK: Butterworth-Heinemann, 1997.
26. Kresta SM III, AWE, Dickey DS, Atiemo-Obeng VA, Forum NAM, eds. *Advances in Industrial Mixing: A Companion to the Handbook of Industrial Mixing*, 2nd Revised ed. Hoboken, NJ: Wiley-Blackwell, 2015.
27. Rushton JH, Costich EW, Everett HJ. Power characteristics of mixing impeller I and II. *Chem Eng Prog*. 1950;46(8):395.
28. Gabriele A, Tsoligkas AN, Kings IN, Simmons MJH. Use of PIV to measure turbulence modulation in a high throughput stirred vessel with the addition of high Stokes number particles for both up- and down-pumping configurations. *Chem Eng Sci*. 2011;66(23):5862–5874.
29. Unadkat H, Nagy ZK, Rielly CD. Investigation of turbulence modulation in solid–liquid suspensions using parallel competing reactions as probes for micro-mixing efficiency. *Chem Eng Res Des*. 2013; 91(11):2179–2189.
30. Mandø M, Lightstone MF, Rosendahl L, Yin C, Sørensen H. Turbulence modulation in dilute particle-laden flow. *Int J Heat Fluid Flow*. 2009;30(2):331–338.
31. Gore RA, Crowe CT. Effect of particle size on modulating turbulent intensity. *Int J Multiph Flow*. 1989;15(2):279–285.
32. Agrawal YK. Towards turbulence modulation in concentrated solid-liquid flows. Masters Thesis, University of Alberta, 2016.

Manuscript received July 24, 2017, and revision received Jan. 15, 2018.